Int. J. Electrochem. Sci., 8 **(2013)** 3974 - 3987

International Journal of
ELECTROCHEMICAL
SCIENCE
www.electrochemsci.org

Electrochemical Evaluation of Environmentally Friendly Cerium Salt as Corrosion Inhibitor for Steel in 3.5 % NaCl

K. F. Khaled[1,2,*]

[1]Materials and Corrosion Laboratory, Chemistry Department, Faculty of Science ,Taif University,Taif, Hawiya 888, Kingdom of Saudi Arabia
[2]Electrochemistry Research Laboratory, Chemistry Department, Faculty of Education, Ain Shams University, Roxy, Cairo, Egypt
*E-mail: khaledrice2003@yahoo.com

Received: 24 January 2013 / *Accepted:* 13 February 2013 / *Published:* 1 March 2013

The inhibition effect of cerium sulphate tetrahydrate on the corrosion of steel in 3.5 % NaCl solutions at 25 ±1 °C was investigated by using electrochemical frequency modulation EFM, electrochemical impedance spectroscopy EIS, potentiodynamic polarization and atomic force microscopy (AFM). The electrochemical measurements demonstrated that, under the chosen experimental conditions cerium sulphate tetrahydrate offers sufficient inhibition against steel corrosion in 3.5% NaCl solutions. EFM can be used as a rapid and non destructive technique for corrosion rate measurements without prior knowledge of Tafel constants. The results of EIS indicate that the value of constant phase element, CPE tends to decrease and both charge transfer resistance and inhibition efficiency tend to increase by increasing the inhibitor concentration. Tafel polarization studies have shown that the cerium sulphate tetrahydrate suppresses both the cathodic and anodic processes and thus it acts as mixed-type inhibitor. AFM analysis shows that the steel surface roughness is 123.08 nm before immersion in the solution, increases to 564.78 nm after immersion in uninhibited solution,. In the presence of the cerium sulphate tetrahydrate, the height profiles of the steel surface decrease to 65.34 nm owing to the protective formation of an inhibitor layer .

Keywords: Corrosion inhibition; Rare Earth salts; EFM; EIS

1. INTRODUCTION

There is an intense research effort to replace chromate because of their toxic nature. Chromium hexavalent compounds, mainly chromates, are widely applied as corrosion inhibitors in aqueous media. Their high efficiency cost ratio has made them standard corrosion inhibitors[1]. Nevertheless, due to their oxidising nature, chromate concentration in the medium must be periodically checked, in

order to avoid undesirable corrosion results, since concentrations lower than a critical value can promote a pitting corrosion process[2-4]. Environmental regulations in industrialized countries are increasing the pressure to eliminate, in the short term, a number of compounds widely used in industrial coatings to prevent corrosion. Hexavalent chromium-based processes are one of the most affected by these regulations. A number of green alternatives to chromates are currently emerging, oriented primarily towards minimizing environmental impact and, secondarily, towards providing effective corrosion inhibition[5, 6].

In this regard, rare earth salts have been tested as corrosion inhibitors for different metal alloys[7-18]. Rare earth inhibitors can be used as pigments in paints for different alloy systems like aluminum alloys, zinc, bronze , steels , and composite [12, 19, 20]. These inhibitors work well in high pH condition and therefore they can be used in alkaline environment[19]. A significant amount of research work is underway to replace chromate by cerium salts [21-23]. Rare earth (RE) ions have a low toxicity [24], and can be considered as economically competitive products [25].

In this work, we report the successful use of cerium sulphate tetrahydrate as eco-friendly corrosion inhibitor for corrosion of steel in 3.5 % NaCl solutions by using several electrochemical techniques include : electrochemical frequency modulation, electrochemical impedance spectroscopy and potentiodynmaic polarization; corrosion kinetic parameters were evaluated and surface topology was studied using atomic force microscope AFM.

2. EXPERIMENTAL SETUP

The experiments were carried out using steel specimens with composition (C = 0.12 wt %, S = 0.04 wt %, Si = 0.015 wt %, Mn = 0.8 wt %, and Fe = balance).

A steel rod of the same composition was mounted in Teflon with an exposed area of 0.28 cm^2 used for potentiodynamic polarization, electrochemical impedance EIS, and electrochemical frequency modulation, EFM measurements.

Inhibitors compounds were obtained from Aldrich chemical co. they were added to the corrosive medium (3.5 % NaCl) at concentrations of 100, 300, 700, 900 mg/l.

Electrochemical experiments were carried out using a conventional electrolytic cell with three-electrode arrangement: saturated calomel reference electrode (SCE), platinum mesh as a counter electrode, and the steel working electrode (WE) had the form of a rod . The counter electrode was separated from the working electrode compartment by fritted glass. The reference electrode was connected to a Luggin capillary to minimize IR drop. Solutions were prepared from bidistilled water of the resistivity 13 MΩcm, Prior to each experiment, the specimen was polished with a series of emery papers of different grit sizes up to 0000 grit size, polished with Al_2O_3 (0.5 mm particle size), washed several times with bidistilled water then with acetone and dried using a stream of air. The electrode potential was allowed to stabilize 60 min before starting the measurements. All experiments were conducted at 25 ±1 °C. The exposed electrode area to the corrosive solution is 0.28 cm^2.

Potentiodynamic polarization curves were obtained by changing the electrode potential automatically from (-700 to -250 mV *vs* SCE) at open circuit potential with scan rate of 0.1 mV s^{-1}.

EIS measurements were carried out in a frequency range of 100 kHz to 40 mHz with amplitude of 5 mV peak-to-peak using ac signals at open circuit potential.

Electrochemical frequency modulation, EFM, was carried out using two frequencies 2 Hz and 5 Hz. The base frequency was 1 Hz, so the waveform repeats after 1 second. The higher frequency must be at least two times the lower one. The higher frequency must also be sufficiently slow that the charging of the double layer does not contribute to the current response. Often, 10 Hz is a reasonable limit.

Measurements were performed with a Gamry Instrument Potentiostat/Galvanostat/ZRA. This includes a Gamry Framework system based on the ESA400, Gamry applications that include DC105 for dc corrosion measurements, EIS300 for electrochemical impedance spectroscopy measurements to calculate the corrosion current and the Tafel constants along with a computer for collecting the data. Echem Analyst 5.58 Software was used for plotting, graphing and fitting data.

Atomic force microscopy (AFM) measurements were performed with a commercial AFM (VEECO). The force curves were measured in contact mode using Si_3N_4 tips with spring constant of 0.02 N/m and the imaging process were performed in tapping mode using Si tips with spring constant of 3 N/m. The samples were immersed in test solutions for 2 h, and then they were taken out of the electrolytes and slightly rinsed with distilled water.

3. RESULTS AND DISCUSSION

Experiments were made using EFM, EIS and potentiodynamic polarization on steel electrode in 3.5 % NaCl open to air.

3.1 EFM measurements

In EFM measurement a potential perturbation signal composed of two sine waves is applied. However, additional and higher frequencies will be obtained in the response of this applied signal due to non-linear nature of corrosion phenomena as shown in Fig. 1.

The EFM intermodulation spectra presented in Fig. 1 (spectra of current response as a function of frequency) were constructed for steel in aerated stagnant 3.5 % NaCl solutions without and with various concentrations of cerium sulphate tetrahydrate at 25 ± 1 °C; A mathematical analysis of these current components at different frequencies can provide the corrosion rate and Tafel parameters for the corroding specimen. Corrosion kinetic parameters listed in Table 1 are calculated from EFM measurements using the following equations:

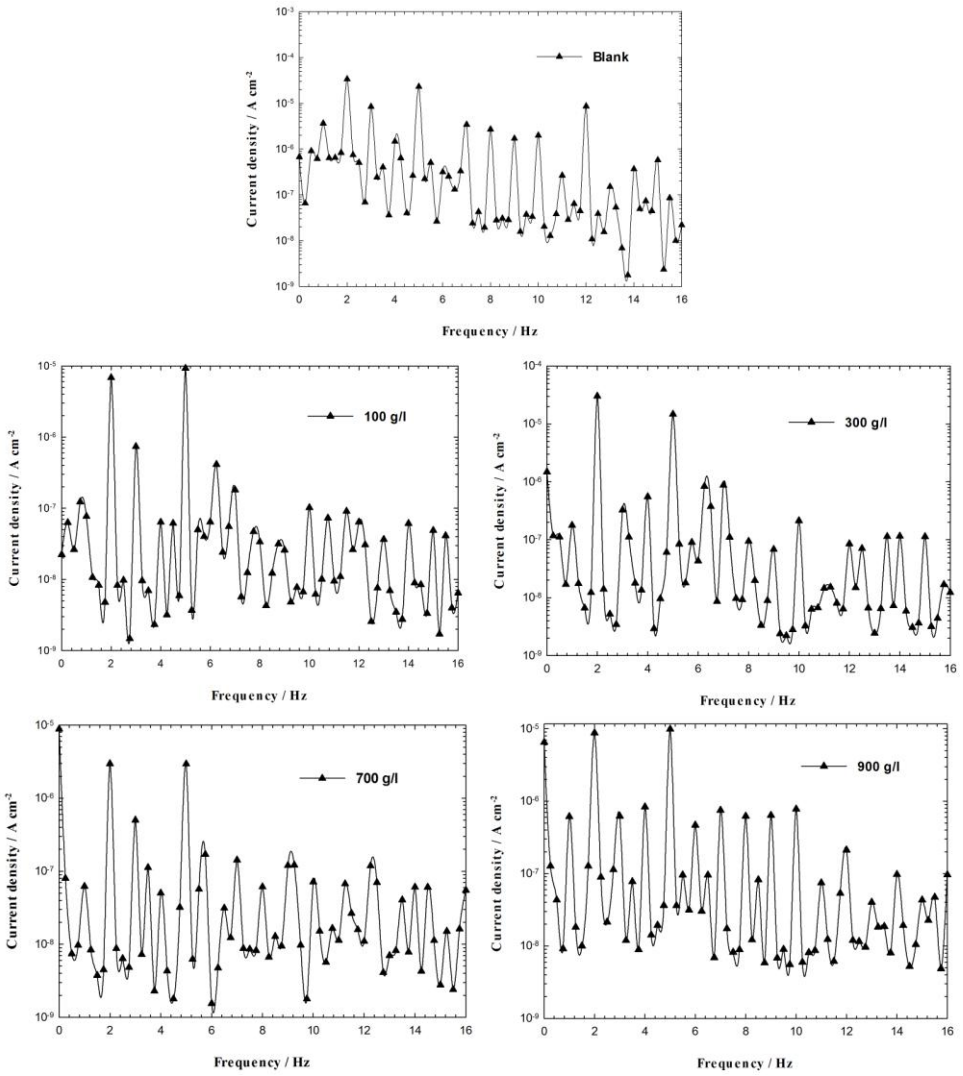

Figure 1. Intermodulation spectra for steel in 3.5 % NaCl in the absence and presence of various concentrations of cerium sulphate tetrahydrate.

$$i_{corr} = \frac{i_{\omega}^{2}}{\sqrt{48\left(2i_{\omega}i_{3\omega} - i_{2\omega}\right)}} \quad (1)$$

$$\beta_a = \frac{i_{\omega}U_o}{2i_{2\omega} + 2\sqrt{3}\sqrt{2i_{3\omega}i_{\omega} - i_{2\omega}^{2}}} \quad (2)$$

$$\beta_c = \frac{i_{\omega}U_o}{2\sqrt{3}\sqrt{2i_{3\omega}i_{\omega} - i_{2\omega}^{2} - 2i_{2\omega}}} \quad (3)$$

$$\text{Causality factor (2)} = \frac{i_{\omega_2 \pm \omega_1}}{i_{2\omega_1}} = 2.0 \quad (4)$$

$$\text{Causality factor (3)} = \frac{i_{2\omega_2 \pm \omega_1}}{i_{3\omega_1}} = 3.0 \qquad (5)$$

where i is the instantaneous current density at the working steel electrode measured at frequency ω and U_o is the amplitude of the sine wave distortion

Table 1. Electrochemical kinetic parameters, inhibition efficiency recorded for steel in 3.5% NaCl solutions without and with various concentrations of (Cerium sulphate tetrahydrate) at 25 ±1 °C calculated by EFM method

Conc. mg/l	i_{corr} μA.cm^{-2}	b_a mV.dec^{-1}	$-b_c$ mV.dec^{-1}	E_{EFM} %	C.F-2	C.F-3
0.00	112.3	100.7	138.2	----	1.94	2.87
100	88.3	139.7	145.7	21.37	199.8	2.99
300	69.06	145.2	189.6	38.50	2.01	2.87
700	56.93	89.7	167.3	49.30	178.9	2.79
900	46.49	102.3	144.0	58.60	1.59	2.88

Table 1 shows the corrosion kinetic parameters such as inhibition efficiency (E_{EFM} %), corrosion current density (μA/cm^2), Tafel constants (b_a , b_c) and causality factors (CF-2, CF-3) at different concentration of cerium sulphate tetrahydrate in 3.5% NaCl at 25 ± 1 °C.

It is obvious from Table 1 that, the corrosion current densities decrease by increasing the concentrations of cerium sulphate tetrahydrate. The causality factors in Table 1 are very close to theoretical values which according to the EFM theory [26, 27] should guarantee the validity of Tafel slopes and corrosion current densities. Inhibition efficiency (E_{EFM}%) depicted in Table 1 calculated from the following equation.

$$E_{EFM}\,\% = (1 - \frac{i_{corr}}{i^{o}_{corr}}) \times 100 \qquad (6)$$

where i^{o}_{corr} and i_{corr} are corrosion current density calculated from equation 1, in the absence and presence of cerium sulphate tetrahydrate, respectively.

As can be seen from Table 1, the corrosion current densities decrease with increase in cerium sulphate concentrations. The causality factors in Table 1 indicate that the measured data are of good quality. The standard values for CF-2 and CF-3 are 2.0 and 3.0, respectively. The causality factor is calculated from the frequency spectrum of the current response (equations 4 and 5). If the causality factors differ significantly from the theoretical values of 2.0 and 3.0, then it can be deduced that the measurements are influenced by noise. If the causality factors are approximately equal to the predicted

values of 2.0 and 3.0, there is a causal relationship between the perturbation signal and the response signal. Then the data are assumed to be reliable [28]. When CF-2 and CF-3 are in the range 0–2 and 0–3, respectively, then the EFM data is valid.

The great strength of the EFM is the causality factors which serve as an internal check of the validity of the EFM measurement [29-31] . With the causality factors the experimental EFM data can be verified.

3.2 Impedance measurements

Impedance spectra for steel in 3.5% NaCl solutions, without and in the presence of different concentrations of cerium sulphate tetrahydrate, were similar in shape. The shape of the impedance diagrams of steel in 3.5% NaCl is similar to those found in the literature [32-35]. The presence of cerium sulphate tetrahydrate increases the impedance but does not change the other aspects of corrosion mechanism occurred due to its addition.

Table 2. Electrochemical parameters calculated from EIS measurements on steel electrode in 3.5 % NaCl solutions without and with various concentrations of (Cerium sulphate tetrahydrate) at 25 ±1 °C.

Conc. mg/l	R_s $\Omega.cm^2$	R_p $\Omega.cm^2$	*CPE* $\mu\Omega^{-1}cm^{-2}S^n$	n	E_{IMP} %
0.00	2.3	79	38.1	0.78	----
100	1.3	111.3	25.9	0.81	29.02
300	2.1	158.9	21.8	0.76	50.28
700	2.4	196.6	20.8	0.79	59.81
900	1.9	280.1	19.7	0.75	71.79

Figure 2 shows the complex plane impedance plots for steel in 3.5% NaCl without and with different concentrations of cerium sulphate tetrahydrate. The parameters obtained by fitting the experimental data presented in Fig. 2 using the equivalent circuit depicted in Fig. 3, and the calculated inhibition efficiencies are listed in Table 2, where R_s represents the solution resistance, R_p is the polarization resistance and can be defined also as the charge-transfer resistance and CPE is a constant phase element. The complex plane impedance plots presented in Fig. 2 clearly demonstrate that the shapes of these plots for inhibited steel electrode are not substantially different from those of uninhibited electrode. Addition of cerium sulphate tetrahydrate molecules increases the impedance but does not change other aspects of the electrode behaviour. complex plane impedance spectra presented in Fig. 2 are modeled using an equivalent circuit model similar to the one proposed by several authors [36-38].

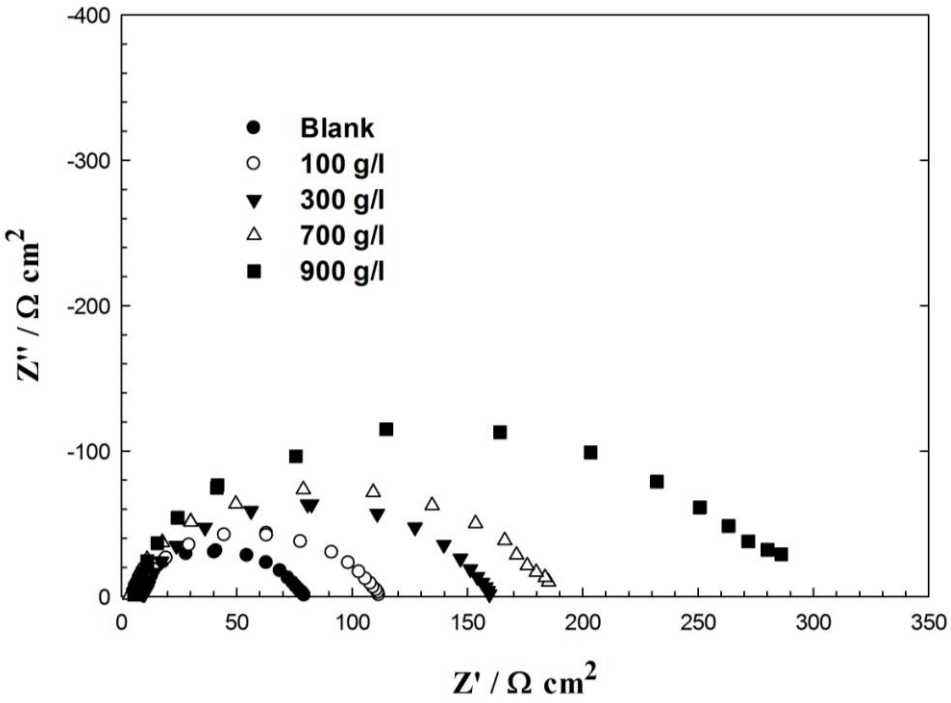

Figure 2. Measured complex plane impedance plots of steel corrosion in 3.5 % NaCl solutions at E_{corr} in the absence and presence of cerium sulphate tetrahydrate at 25 ±1 °C.

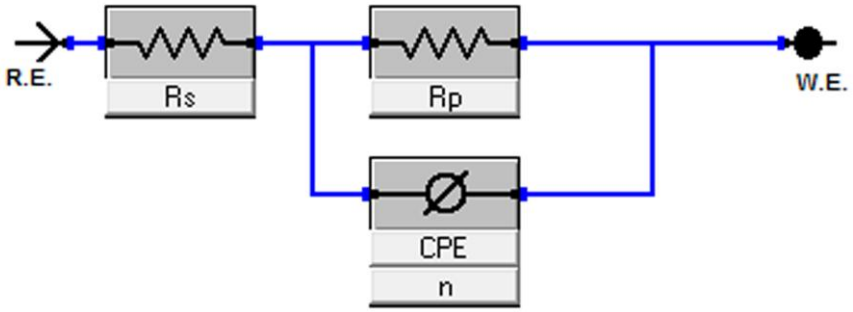

Figure 3. Equivalent circuit model for steel /3.5% NaCl interface

The impedance spectra obtained for steel in 3.5% NaCl contains depressed semicircle with the center under the real axis, such behaviour is characteristic for solid electrodes and often referred to as frequency dispersion and attributed to the roughness and other inhomogenities of the solid electrode [39-41].

Parameters derived from EIS measurements and inhibition efficiency is given in Table 2. Addition of cerium sulphate tetrahydrate increases the values of R_p and lowers the values of CPE and this effect is seen to be increased as the concentrations of cerium sulphate tetrahydrate increase. The constant phase element (CPE) with their n values $1 > n > 0$ represent double layer capacitors with

some pores [42]. The CPE decreases upon increase in cerium sulphate tetrahydrate concentrations, which are expected to cover the charged surfaces and reducing the capacitive effects.

This decrease in (CPE) results from a decrease in local dielectric constant and/or an increase in the thickness of the double layer, suggested that cerium sulphate tetrahydrate molecules inhibit the steel corrosion by adsorption at the steel/NaCl interface The semicircles in Fig. 2 are generally associated with the relaxation of electrical double layer capacitors and the diameters of these semicircles can be considered as the charge-transfer resistance ($R_{ct} = R_p$) [31]. Therefore, the inhibition efficiency, $E_{IMP}\%$ of cerium sulphate tetrahydrate for the steel electrode can be calculated from the polarization resistance as follows [43]:

$$E_{IMP}\% = (1 - \frac{R_p^o}{R_p}) \times 100 \qquad (7)$$

where R_p^o and R_p are the polarization resistances for uninhibited and inhibited solutions, respectively.

3.3 Potentiodynamic polarization measurements

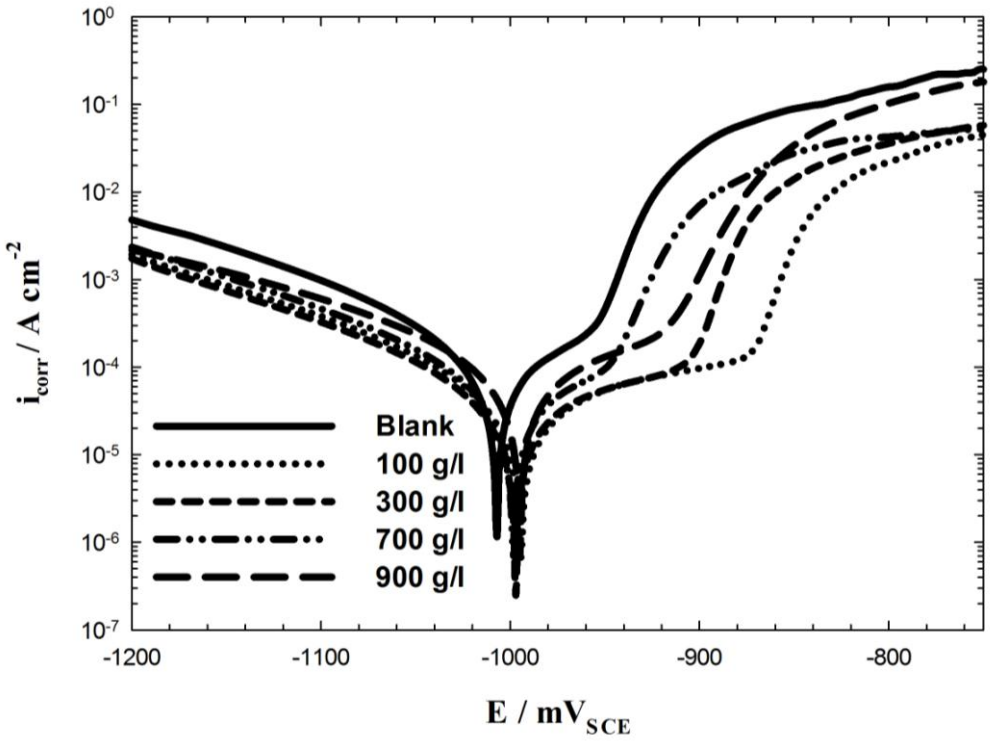

Figure 4. Anodic and cathodic Tafel polarization curves for mild steel in the absence and presence of various concentrations of cerium sulphate tetrahydrate in 3.5% NaCl at 25 ±1 °C.

Measurements of current-potential values under carefully controlled conditions can yield information on corrosion rates, coatings and films, passivity, pitting tendencies and other important phenomena.

Figure 4 represents the anodic and cathodic potentiodynamic polarisation curves of steel in 3.5 % NaCl solutions in the absence and the presence of various concentrations of cerium sulphate tetrahydrate. Inspection of Fig. 4 reveals that E_{corr} values in the presence of inhibitor have no definite shift which indicate that this inhibitor acts as mixed-type inhibitor. Regarding the polarisation curves, the addition of cerium sulphate tetrahydrate has a pronounced effect on both the cathodic and anodic parts of the polarisation curves. A limiting diffusion current appears at higher overvoltage on the anodic polarisation curves of steel in 3.5 % NaCl solutions in the absence and the presence of various concentrations of cerium sulphate tetrahydrate shows that charge transfer towards the electrode surface becomes the rate determining step.

The relatively lower inhibition efficiencies of cerium salt, recorded by potentiodynamic polarization techniques are due to the adsorption of the Ce^{+4} in its hydrated state, where the main oxidizing – reducing reactions are listed as follow [44]:

$$Ce^{4+} + Fe^{2+} \rightarrow Ce^{3+} + Fe^{3+} \quad (8)$$

$$2Fe^{3+} + Fe \rightarrow 3Fe^{2+} \quad (9)$$

$$2Ce^{4+} + Fe \rightarrow 2Ce^{3+} + Fe^{2+} \quad (10)$$

The reactions indicated that Ce^{4+} and Fe^{3+} (produced as a result of the above reactions, have a depolarizing effect on the anodic reaction rate and accelerate the dissolution of steel in the neutral solution. Furthermore, the standard electrode potential of Ce^{3+}/Ce ($-2.48\ V_{SHE}$) is much lower than that of Fe^{2+}/Fe ($-0.441\ V_{SHE}$), so it is impossible for the cerium ion (Ce^{4+} and Ce^{3+}) to precipitate onto the steel surface [44].

Table 3. Electrochemical parameters calculated from polarization measurements on the steel electrode in 3.5 % NaCl solutions without and with various concentrations of (cerium sulphate tetrahydrate) at 25 ±1 °C.

Conc. mg/l	i_{corr} $\mu A.cm^{-2}$	$-E_{corr}$ mV	b_a $mV.dec^{-1}$	$-b_c$ $mV.dec^{-1}$	C.R mpy	E_T %
0.00	92.15	1007	68.6	109	39.53	----
100	68.55	994.5	333.1	139.3	29.40	25.61
300	52.0	997.1	221.1	130.6	22.3	43.57
700	41.14	998.2	74.65	111.1	17.65	55.35
900	34.26	994.4	63.34	113.6	14.7	62.82

Table 3 shows the electrochemical corrosion kinetic parameters, i.e. corrosion potential (E_{corr}), cathodic and anodic Tafel slopes (b_c, b_a) and corrosion current density i_{corr} obtained by extrapolation of the Tafel lines. The calculated inhibition efficiency, $E_T\%$ are also reported from equation (11),

$$E_T\% = (1 - \frac{i_{corr}}{i^o_{corr}}) \times 100 \qquad (11)$$

where i^o_{corr} and i_{corr} are corrosion current density in the absence and presence of cerium sulphate tetrahydrate, respectively. The best inhibition efficiency was about 62.8% (900 mg/l). It can be seen that by increasing inhibitor concentration, the corrosion rate decreased and inhibition efficiency $E_T\%$, increased.

3.4. AFM observations

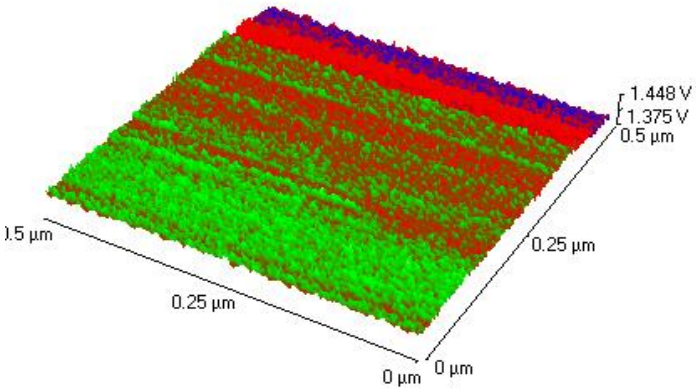

Figure 5. AFM three-dimensional images of steel surface after 6 h of immersion at 25 ±1 °C in 3.5 % NaCl

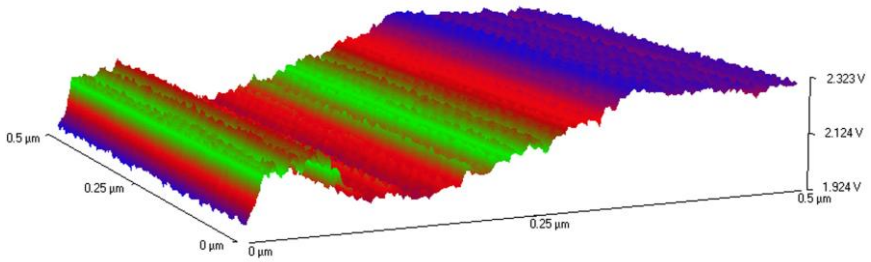

Figure 6. AFM three-dimensional images of steel surface after 6 h of immersion at 25 ±1 °C in 3.5 % NaCl + 900 mg/l cerium salt.

Figures 5 and 6 are the three-dimensional AFM images of steel surface in absence and presence of cerium sulphate tetrahydrate, respectively. Inspection of these figures reveal that the sample before immersion has a regular surface with certain imperfections as a result of the abrading

treatment. Figure 7 shows the steel surface roughness as a consequence of the large amount of corrosion products formed on the metallic surface, the steel surface roughness is 123.08 nm before immersion in the solution, increases to 564.78 nm after immersion in uninhibited solution,. In the presence of the cerium sulphate tetrahydrate, the height profiles of the steel surface decrease to 65.34 nm owing to the protective formation of an inhibitor layer . These results prove that the cerium sulphate tetrahydrate inhibitor can inhibit steel corrosion.

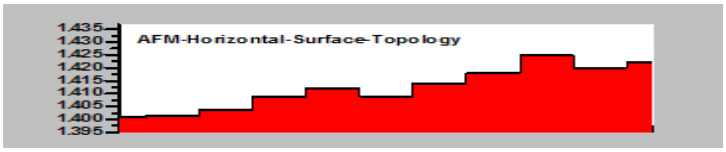

Figure 7. AFM horizontal surface topology for steel in 3.5% NaCl.

3.5. Mechanism of inhibition

It is well known that the cathodic reaction for metals in aerated neutral solutions is the oxygen reduction according to equation 12,

$$O_2 + 2H_2O + 4e^- \rightarrow 4OH^- \quad (12)$$

This process consumes the electrons that are released during the oxidation reaction, where the corrosion of iron can undergo two different transformations as follows

$$Fe \rightleftarrows Fe^{2+} + 2e^- \quad (13)$$

$$Fe^{2+} \rightleftarrows Fe^{3+} + e^- \quad (14)$$

Nevertheless, in practice the second transformation, equation 14, will not occur. While the dissolution of iron in concentrated NaCl solutions into ferrous cations can be explained according to Darwish et al. [45, 46]

$$Fe + H_2O \rightleftarrows Fe(OH)_{ads} + H^+ \quad (15)$$

$$Fe(Cl^-)_{ads} + Fe(OH)_{ads} \rightleftarrows Fe + FeOH^+ + (Cl^-) + 2e^- \quad (16)$$

$$FeOH^+ + H^+ \rightleftarrows Fe^{2+}_{aq} + H_2O \quad (17)$$

In addition, the hydroxide ions resulting from equation 1 will react with Fe_{aq}^{2+} to form a deposit of $Fe(OH)_2$,

$$Fe+ \tfrac{1}{2} O_2 + H_2O \rightleftharpoons Fe(OH)_2 \quad (18)$$

If there is an excess of oxygen presented, the formed ferrous hydroxide transforms to the final corrosion product that is called magnetite (Fe_3O_4) according to the following reaction,

$$3Fe(OH)_2 + \tfrac{1}{2} O_2 \rightleftharpoons Fe_3O_4 + 3H_2O \quad (20)$$

The following is the suggested inhibition mechanism presented Based on the electrochemical polarization described above, surface analytical data and from our theoretical study described elsewhere[47]., it is possible to surmise the following mechanism for inhibition by rare metal salts [48]:

$$Fe \rightarrow Fe^{2+} + 2e^- \quad (21)$$

$$O_2 + 2H_2O + 4e^- \rightarrow 4OH^- \quad (22)$$

$$Ce^{4+} + Fe^{2+} \rightarrow Ce^{3+} + Fe^{3+} \quad (23)$$

$$Fe^{2+} + 2OH^- \rightarrow Fe(OH)_2 \quad (24)$$

$$Fe(OH)_2 \xrightarrow{O_2} Fe(OH)_3 \rightarrow Fe_2O_3 \quad (25)$$

$$Ce^{3+} + 3OH^- \rightarrow Ce(OH)_3 \rightarrow Ce_2O_3 \quad (26)$$

4. CONCLUSION

The main conclusions of the present study can be summarized as follows:

- The electrochemical measurements demonstrated that cerium sulphate tetrahydrate offers inhibition against steel corrosion in 3.5% NaCl solutions.
- EFM can be used as a rapid and non destructive technique for corrosion rate measurements without prior knowledge of Tafel constants.
- The results of EIS indicate that the value of CPEs tends to decrease and both charge transfer resistance and inhibition efficiency tend to increase by increasing the inhibitor concentration.
- Tafel polarization studies have shown that the cerium sulphate tetrahydrate suppresses both the cathodic and anodic processes and thus it acts as mixed-type inhibitor.
- AFM analysis shows the steel surface roughness is decreased upon addition of cerium sulphate tetrahydrate.

ACKNOWLEDGMENTS
Author would like to thank King Abdulaziz City for Science and Technology, KACST for the financial support of this work provided through project # AT-30-66 titled" Development of a new corrosion protection strategy for water-ammonia refrigerating systems ". Author is thankful to the AFM personnel in the AFM unit at Taif University.

References

1. W. Wittke, *J. Met. Finishing*, 87 (1989) 24.
2. L.F.G. Williams, *Corros. Sci.*, 13 (1973) 865-868.
3. C. Lemaitre, B. Baroux, G. Beranger, *Werkstoffe und Korrosion*, 40 (1989) 229-236.
4. A. Bahadur, *Mater. Trans., JIM*, 34 (1993) 1191-1194.
5. M. Bethencourt, F.J. Botana, J.J. Calvino, M. Marcos, M.A. RodrÍguez-Chacón, *Corros. Sci.*, 40 (1998) 1803-1819.
6. A. Aballe, M. Bethencourt, F.J. Botana, M.J. Cano, M. Marcos, *Materials and Corrosion-Werkstoffe Und Korrosion*, 52 (2001) 344-350.
7. D.-Q. Zhang, H. Wu, L.-X. Gao, *Mater. Chem. Phys.*, 133 (2012) 981-986.
8. F. Mert, C. Blawert, K.U. Kainer, N. Hort, *Corros. Sci.*, 65 (2012) 145-151.
9. E.A. Matter, S. Kozhukharov, M. Machkova, V. Kozhukharov, *Corros. Sci.*, 62 (2012) 22-33.
10. T.H. Muster, H. Sullivan, D. Lau, D.L.J. Alexander, N. Sherman, S.J. Garcia, T.G. Harvey, T.A. Markley, A.E. Hughes, P.A. Corrigan, A.M. Glenn, P.A. White, S.G. Hardin, J. Mardel, J.M.C. Mol, *Electrochim. Acta*, 67 (2012) 95-103.
11. J. Yan, Y. Gao, Y. Shen, F. Yang, D. Yi, Z. Ye, L. Liang, Y. Du, *Corros. Sci.*, 53 (2011) 3588-3595.
12. A.K. Mishra, R. Balasubramaniam, *Corrosion*, 63 (2007) 240-248.
13. T.H. Muster, D. Lau, H. Wrubel, N. Sherman, A.E. Hughes, T.G. Harvey, T. Markley, D.L.J. Alexander, P.A. Corrigan, P.A. White, S.G. Hardin, M.A. Glenn, J. Mardel, S.J. Garcia, J.M.C. Mol, *Surf. Interface Anal.*, 42 (2010) 170-174.
14. A.L. Rudd, C.B. Breslin, F. Mansfeld, *Corros. Sci.*, 42 (2000) 275-288.
15. X. Li, S. Deng, H. Fu, G. Mu, N. Zhao, *Appl. Surf. Sci.*, 254 (2008) 5574-5586.
16. B.R.W. Hinton, *J. Alloys Compd.*, 180 (1992) 15-25.
17. B. Davó, J.J. de Damborenea, *Electrochim. Acta*, 49 (2004) 4957-4965.
18. M. Tran, D. Mohammedi, C. Fiaud, E.M.M. Sutter, *Corros. Sci.*, 48 (2006) 4257-4273.
19. A.K. Mishra, R. Balasubramaniam, *Mater. Chem. Phys.*, 103 (2007) 385-393.
20. A.K. Mishra, R. Balasubramaniam, *Corros. Sci.*, 49 (2007) 1027-1044.
21. F.B. Mansfeld, Z. Sun, Inhibition of steel corrosion in ammonia/water heat pump, involves introducing rare earth metal salts to the working fluid, in, Advanced Mechanical Technology Inc.
22. J.D. Gorman, A.E. Hughes, D. Jamieson, P.J.K. Paterson, *Corros. Sci.*, 45 (2003) 1103-1124.
23. A. Amadeh, S.R. Allahkaram, S.R. Hosseini, H. Moradi, A. Abdolhosseini, *Anti-Corros Method M.*, 55 (2008) 135-143.
24. A.K. Mishra, R. Balasubramaniam, S. Tiwari, *Anti-Corros Method M.*, 54 (2007) 37-46.
25. B. Claux, J. Serp, J. Fouletier, *Electrochim. Acta*, 56 (2011) 2771-2780.
26. K.F. Khaled, *Mater. Chem. Phys.*, 112 (2008) 290-300.
27. K.F. Khaled, *J. Appl. Electrochem.*, 39 (2009) 429-438.
28. R.W. Bosch, F. Moons, J.H. Zheng, W.F. Bogaerts, *Corrosion*, 57 (2001) 532-539.
29. S.S. Abdel-Rehim, K.F. Khaled, N.S. Abd-Elshafi, *Electrochim. Acta*, 51 (2006) 3269-3277.
30. E. Kuş, F. Mansfeld, *Corros. Sci.*, 48 (2006) 965-979.
31. K.F. Khaled, N.S. Abdel-Shafi, N.A. Al-Mobarak, *Int. J. Electrochem. Sci*, 7 (2012) 1027-1044.
32. K.F. Khaled, N. Hackerman, *Mater. Chem. Phys.*, 82 (2003) 949-960.

33. K.F. Khaled, S.S. Abd El Rehim, N. Hackerman, 2003.
34. K.F. Khaled, N.A. Al-Mobarak, *Int. J. Electrochem. Sci*, 7 (2012) 1045-1059.
35. K.F. Khaled, *Mater. Chem. Phys.*, 130 (2011) 1396-1396.
36. K.F. Khaled, S.S. Abdel-Rehim, G.B. Sakr, *Arabian Journal of Chemistry*, 5 (2012) 213-218.
37. K.F. Khaled, *J. Electrochem. Soc.*, 158 (2011) S28-S28.
38. L. Han, S. Song, *Corros. Sci.*, 50 (2008) 1551-1557.
39. H. Ma, S. Chen, L. Niu, S. Zhao, S. Li, D. Li, *J. Appl. Electrochem.*, 32 (2002) 65-72.
40. K.F. Khaled, N.A. Al-Mobarak, *Int. J. Electrochem. Sci*, 7 (2012) 1045-1059.
41. Zarrouk, B. Hammouti, H. Zarrok, M. Bouachrine, K.F. Khaled, S.S. Al-Deyab, *Int. J. Electrochem. Sci*, 7 (2012) 89-105.
42. E.M. Sherif, S.M. Park, *Electrochim. Acta*, 51 (2006) 1313-1321.
43. K.F. Khaled, S.S. Abdel-Rehim, G.B. Sakr, *Arabian Journal of Chemistry*, 5 (2012) 213-218.
44. X. Li, S. Deng, H. Fu, G. Mu, *Corros. Sci.*, 52 (2010) 1167-1178.
45. N.A. Darwish, F. Hilbert, W.J. Lorenz, H. Rosswag, *Electrochim. Acta*, 18 (1973) 421-425.
46. E.-S.M. Sherif, *Int. J. Electrochem. Sci*, 6 (2011) 3077-3092.
47. K.F. Khaled, N.S. Abdelshafi, A. El-Maghraby, N.A. Al-Mobarak, *J. Mater. Envron. Sci.*, 2 (2011) 166-173.
48. V.S. SASTRI, Green Corrosion Inhibitors : Theory and Practice, John Wiley & Sons, Inc.,, 2011.